MIT Libraries | DSpace@MIT

MIT Open Access Articles

Front-electrode design for efficient near-field thermophotovoltaics

The MIT Faculty has made this article openly available. ***Please share*** how this access benefits you. Your story matters.

Citation:

Published Version: 10.1117/12.2529736

Publisher: SPIE-Intl Soc Optical Eng

Permanent Link: https://hdl.handle.net/1721.1/132455

Version: Final published version: final published article, as it appeared in a journal, conference proceedings, or other formally published context

Terms of use: Article is made available in accordance with the publisher's policy and may be subject to US copyright law. Please refer to the publisher's site for terms of use.

Massachusetts Institute of Technology

PROCEEDINGS OF SPIE

SPIEDigitalLibrary.org/conference-proceedings-of-spie

Front-electrode design for efficient near-field thermophotovoltaics

Karalis, Aristeidis, Joannopoulos, John

Aristeidis Karalis, John D. Joannopoulos, "Front-electrode design for efficient near-field thermophotovoltaics," Proc. SPIE 11081, Active Photonic Platforms XI, 1108127 (5 September 2019); doi: 10.1117/12.2529736

SPIE.

Event: SPIE Nanoscience + Engineering, 2019, San Diego, California, United States

Downloaded From: https://www.spiedigitallibrary.org/conference-proceedings-of-spie on 30 Oct 2020 Terms of Use: https://www.spiedigitallibrary.org/terms-of-use

Front-electrode design for efficient near-field thermophotovoltaics

Aristeidis Karalis*[a], John D. Joannopoulos[a,b]
[a]Research Laboratory of Electronics, Massachusetts Institute of Technology, Cambridge, MA, 02139, USA; [b]Department of Physics, Massachusetts Institute of Technology, Cambridge, MA, 02139, USA

ABSTRACT

The effects of the necessary front electrode in near-field ultrathin resonant thermophotovoltaic cells are analyzed. Absorption inside the transparent conducting electrode limits the power level that can be efficiently converted to electricity and several electrode materials are compared in performance. The assisting grid of metallic fingers suppresses thermal radiation from the emitter in its region across from them, leading to reduced shading losses and wider optimal fingers than usually associated with far-field photovoltaic cells. Promising performances are predicted, reaching 24% at 900K and 48% at 2100K.

Keywords: thermophotovoltaics, transparent conducting electrodes, radiative heat transfer, plasmonics, thin films

1. INTRODUCTION

1.1 Thermophotovoltaics

The ability to convert heat to electricity is of utmost importance within the quest for green energy technologies. If it could be achieved efficiently for heat emitters of relatively low temperature (<1000ºK), it would allow to harvest waste heat from industrial plants and thus recycle some of their losses. Moreover, since heat can be produced very easily by burning a large variety of fuels (hydrocarbon, nuclear, etc.) or by absorbing the sun irradiation, any heat-to-electricity process can serve to create both power generators and solar cells. Thermodynamics dictates that the limit of efficiency of such a device, comprising the hot emitter at temperature T_e and the cold receptor of heat at temperature T_a, is the Carnot efficiency $\eta_C = 1 - T_a/T_e$. Therefore, operation at extremely high temperatures (>2000ºK) would be beneficial for efficient such generators and cells.

There are multiple methods devised to solve this problem, such as thermoelectrics[1], thermoradiative cells[2] and thermophotovoltaic (TPV) cells[3]. This work concerns thermophotovoltaics, wherein the hot body emits thermal radiation, which is then absorbed by a cold photovoltaic (PV) cell, placed across from the emitter, to convert it to electricity. The premise of this method is that the spectrum of the thermal emission can be tailored to the characteristics of the PV cell, so that the latter operates at a very high efficiency. For this method to work well, the other mechanisms for heat transport between emitter and cell, convection and conduction, must be minimized. Therefore, such TPV cells always operate within vacuum (very low air pressure) inside a sealed enclosure and a gap separates emitter and cell.

1.2 Far-field versus near-field

Naturally, the first implementations of a TPV cell consisted of a sizeable vacuum gap, as it easier to fabricate and maintain in an operational device. Since the majority of TPV losses are due to absorption below the semiconductor band gap, most of the research has been focused on designing selective emitters or reflective filters, so that below-gap thermal radiation is suppressed as much as possible[4,5]. In this far-field case, where the emitter and cell are distant several times the central wavelength of thermal emission, all the radiation reaching the cell consists of propagating waves. Stated differently all modes lie inside the radiation cone. At a given temperature differential, this sets a limit on the power that can be transmitted from the emitter to the cell, known as Planck's thermal radiation limit, and imposes an important design tradeoff: given that the PV cell operates most efficiently for radiation close to its band gap, narrowband radiation would be preferred, but then power emitted within this small bandwidth would be very limited; instead, a broadband thermal spectrum increases the power, but works less efficiently.

Active Photonic Platforms XI, edited by Ganapathi S. Subramania, Stavroula Foteinopoulou,
Proc. of SPIE Vol. 11081, 1108127 · © 2019 SPIE · CCC code: 0277-786X/19/$21
doi: 10.1117/12.2529736

Downloaded From: https://www.spiedigitallibrary.org/conference-proceedings-of-spie on 30 Oct 2020
Terms of Use: https://www.spiedigitallibrary.org/terms-of-use

By bringing the cell close to the near field of the emitter, namely, within a thermal wavelength, also the evanescent modes of the emitter can reach the cell, so they contribute to overall power transmission. Therefore, the Planck power limit can now be broken and there have been demonstrations[6,7] of significant power delivery increase in the near field,

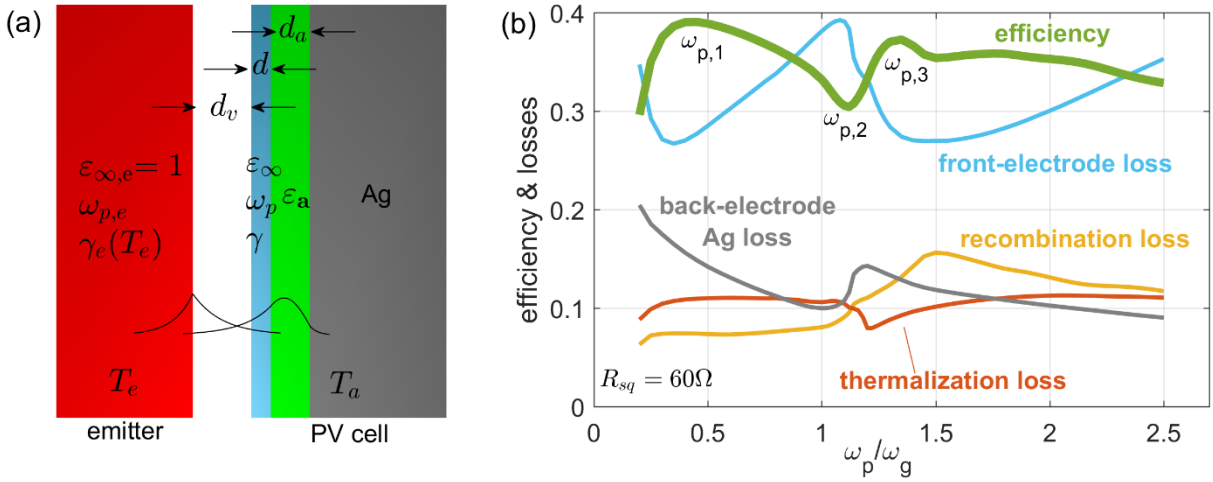

Figure 1. (a) Near-field TPV cell topology with SPP emitter (red) and ultrathin single-mode PV cell, consisting of a front conducting electrode (blue), a semiconductor absorber (green) and a silver back electrode (grey). The modes supported by each unit and their evanescent coupling is indicated. (b) Efficiency and losses as a function of front-electrode doping. Efficiency is maximized at a doping level that makes the electrode transparent, but also opaque operation can be efficient, while a resonant electrode absorbs too many thermal photons.

so this TPV regime of operation has received considerable interest[8-16]. The efficiency versus power tradeoff can also be overcome, as narrowband efficient operation does not also mean limited power.

1.3 Planar surface-plasmon-polariton emitters with ultrathin cells for narrowband near-field emission in a practical implementation[17]

In previous work, we had proposed a material and geometry system that achieves such narrowband thermal power transmission, with our major intent to boost the TPV efficiency. It consists of a planar metallic emitter, which supports a surface-plasmon-polariton (SPP) mode at its interface with the vacuum gap, and an ultrathin TPV cell, with a semiconductor depletion region thin enough to support only a single photonic waveguide mode, backed by silver as its back electrode and a transparent conducting electrode in the front, as shown in Fig. 1(a). By optimizing the emitter metal plasma frequency, the cell thickness and vacuum gap width, this topology was designed such that the SPP mode of the thermal emitter and the single photonic mode of the cell cross-couple and are impedance matched at a frequency slightly above the semiconductor band gap E_g. This design manages to maximize the emitter thermal emissivity where the cell absorbs efficiently and to minimize it elsewhere, especially below the band gap, so that a narrowband efficient but powerful near-field spectrum can be created.

Apart from the great performance benefits, this topology has important advantages in fabricability. Much work in both far-field and near-field TPV has been devoted to the design of complex periodic emitters, which emit narrowband radiation. However, these structures with complicated nanofeatures cannot easily withstand operation at extremely high temperatures and run the risk of collapsing even if very refractory materials are used[18]. Instead, our proposed structure consisting only of planar films should be able to stay stable up to almost the melting temperature of the refractory metal emitter. The ultrathin cell design has the benefits that one saves considerable cost of the expensive direct band gap material, it can be fabricated with precise epitaxial methods thus avoiding defects, which lead to bulk and surface recombination, and should also be depleted from carriers throughout its tiny thickness, further boosting its internal quantum efficiency. Moreover, the resonant design requires only the evanescent tails of the two modes to couple and thus results in optimized topologies with medium near-field vacuum gaps (~100s of nm), which can be fabricated and maintained much more easily that the tiny (~10nm) gaps associated usually with near-field TPV.

Downloaded From: https://www.spiedigitallibrary.org/conference-proceedings-of-spie on 30 Oct 2020
Terms of Use: https://www.spiedigitallibrary.org/terms-of-use

A crucial conclusion of that work was also that it is absolutely essential to include in the modeling the front electrode, which is necessary to conduct the photo-generated current to the load. It typically consists of a transparent conducting electrode and a grid of metallic fingers. These losses are shown to have an effect in performance and exhibit some interesting behavior, while design guidelines are suggested.

2. TRANSPARENT CONDUCTING ELECTRODES

2.1 Design tradeoffs in far-field PV cells versus near-field TPV cells[19]

The front transparent conducting electrode of a cell has dual, conflicting roles: it needs to have large enough direct-current (dc) conductivity to laterally conduct the photo-generated current to the metallic fingers with few ohmic losses and, at the same time, small enough optical conductivity to allow through the photons to be absorbed by the semiconductor cell with few optical losses[20,21]. Unfortunately, dc and optical conductivities are usually strongly correlated. Therefore, the TCE design optimization boils down mainly to material selection, but it turns out that near-field topologies add extra constraints, nonexistent in far-field cells.

Let us model the optical conductivity of a front TCE with the Drude relative permittivity:

$$\varepsilon(\omega) = \varepsilon_\infty \left(1 - \frac{\omega_p^2}{\omega^2 + \mathrm{i}\gamma\omega}\right), \tag{1}$$

where ε_∞ the short-wavelength limit for the material, ω_p its plasma frequency quantifying mainly the free-carrier density inside it and γ the electron-scattering loss rate. In most conductors (e.g. noble metals), all these parameters are fixed. However, there are engineered materials, whose free-carrier density can be controlled via doping within a certain range, so ω_p is tunable and, naturally, the loss rate depends on the number of carriers with some dependence $\gamma(\omega_p)$.

If we examine the ratio of optical conductivity $\sigma(\omega) = \omega\varepsilon_o \mathrm{Im}\{\varepsilon(\omega)\}$ to the dc conductivity $\sigma(0)$, we find

$$\frac{\sigma(\omega)}{\sigma(0)} = \frac{\gamma^2(\omega_p)}{\gamma^2(\omega_p) + \omega^2}. \tag{2}$$

In far-field PV cells, this relation easily leads to the conclusion that the best TCE performance will be provided by the material and doping level, which gives the smallest $\gamma(\omega_p)$, as long as $\omega_p < \omega$, so that the TCE material is indeed transparent [$\mathrm{Re}\{\varepsilon(\omega)\} > 0$ from Eq.(1)] at the operating frequency ω. Therefore, noble metals (Ag, Au) with very high carrier densities are opaque and thus unusable in the visible and infrared frequency ranges. Instead, for PV cells in the visible, indium-doped tin oxide (ITO) is widely accepted as the best choice, but it would also be opaque in the infrared.

Let us then assume a hypothetical TCE material, whose loss rate increases monotonically with carrier density as $\hbar\gamma = 0.0072eV + 0.04\hbar\omega_p$, the two terms corresponding to phonon (carrier independent) and impurity (carrier dependent) scattering. In Fig. 1(b), we then plot the performance of the near-field TPV cell in Fig. 1(a), with $T_e = 2100°K$, $E_g = 4k_BT_e = 0.72eV$ ($\lambda_g = 1.72\mu m$) and for a constant square resistance $R_{sq} = 60\Omega$ of the TCE, with all the cell parameters ($\omega_{p,e}, d_v, d_a$ and depletion region voltage V) optimized for efficiency. Intuition from far-field PV cells would suggest that efficiency would decrease monotonically with ω_p. What we see instead is a rather complex behavior in efficiency, clearly correlated to the losses inside the front TCE. This can be explained by physical phenomena present in the near field that do not occur for far-field cells: (1) For low doping, the electrode has to become much thicker to maintain the same R_{sq}, but this means increasing the distance of the semiconductor region from the emitter, on which evanescent field coupling mainly relies, so efficiency rapidly decreases. (2) For ω_p roughly equal to the semiconductor band gap frequency ω_g, the SPP resonance supported on the interface between the TCE and the vacuum gap aligns itself with the band gap, where most thermal radiation is peaked, leading to enhanced losses inside the TCE and a drop in efficiency at ω_{p2}. (3) Although maximum efficiency occurs at a doping level $\omega_{p1} < \omega_g$, where the TCE is transparent, there is another local efficiency maximum at $\omega_{p3} > \omega_g$, where the TCE is opaque; since the semiconductor region is ultrathin (for single-mode near-field operation), the emitter evanescent fields sufficiently penetrate into it and lead to photo-generated current. At large doping, the overall expected trend of efficiency decreasing still holds.

Downloaded From: https://www.spiedigitallibrary.org/conference-proceedings-of-spie on 30 Oct 2020
Terms of Use: https://www.spiedigitallibrary.org/terms-of-use

It is quite obvious that the presence of the front TCE plays a significant role in the performance of the TPV cell in the near field and its design involves proper choice of the material and its doping in harmony with the resonant phenomena present in these near-field cells. Low electron scattering loss rates and doping up to transparency are obviously still preferable, but operation with an opaque electrode is still possible, while a resonance of the TCE with the main thermal field should be avoided.

2.2 Does near-field TPV always get better as the vacuum gap is shrunk?

Ever since heat transfer via near-field evanescent waves for TPV was shown to provide benefits in increased power densities, it is customary to see predicted dependencies of both power delivery and efficiency monotonically rise as the vacuum gap gets smaller and the device enters further into the near field[9,14,15]. Since the power exchanged between two planar bodies of different temperatures scales as $\sim 1/d_v^2$, where d_v the vacuum gap in between, extensive research has, in fact, been devoted to determining the limits of power exchange (due to spatial material dispersion from nonlocal effects) between the two materials[22]. However, all these studies ignore the presence of the necessary TCE and its associated losses.

Starting from the solution of optimal efficiency in Fig. 1(b) (at doping ω_{p1} and $d_v/\lambda_g \approx 0.2$), we plot the cell performance with varying vacuum gap width d_v in Fig. 2. As the distance between emitter and cell increases, the system reaches its far-field limit at about one band-gap wavelength λ_g, and power emitted and converted to electricity are fairly constant thereafter, as seen in Fig. 2(b). In the other direction, however, it is quite obvious that efficiency drops drastically, as emitter and cell are brought closely together (to tens of nm distances) and all the associated losses are absorption inside the front TCE. This doesn't violate the notion that more power should be emitted as larger-wavevector evanescent waves are activated. The power emitted indeed increases monotonically as $\sim 1/d_v^2$. The issue is that the power converted to electricity is rather unchanged and, in fact, slightly decreases. All the rest is lost inside the TCE due to its finite R_{sq}[23]. Physically, this behavior is easily explained by the fact that the larger wavevectors associated with smaller vacuum gaps lead to these emitted evanescent modes shrinking more and more in the lateral dimension, localizing closer to the emitter surface. Therefore, they cannot reach deep into the TPV cell and its semiconductor depletion region, instead they mostly penetrate up to the front TCE. If one attempted to use a thinner TCE, to get the desired square resistance R_{sq} more carriers would be needed, which typically signifies higher absorption rate, so the net effect would be the same.

This is likely the single most important message we can draw, by analyzing front TCEs for near-field TPV cells. These electrodes cannot be ignored, as the photo-generated current needs an escape route to the load terminals, especially as these current levels increase in the near field. But then their presence implies clear limits on the power that can be converted and the attainable efficiency. Interestingly, optimal performance is observed at mid-range vacuum gaps of hundreds of nm and not closer, a fact that at least has the positive attribute that such a separation can be more easily fabricated and maintained in practice.

Downloaded From: https://www.spiedigitallibrary.org/conference-proceedings-of-spie on 30 Oct 2020
Terms of Use: https://www.spiedigitallibrary.org/terms-of-use

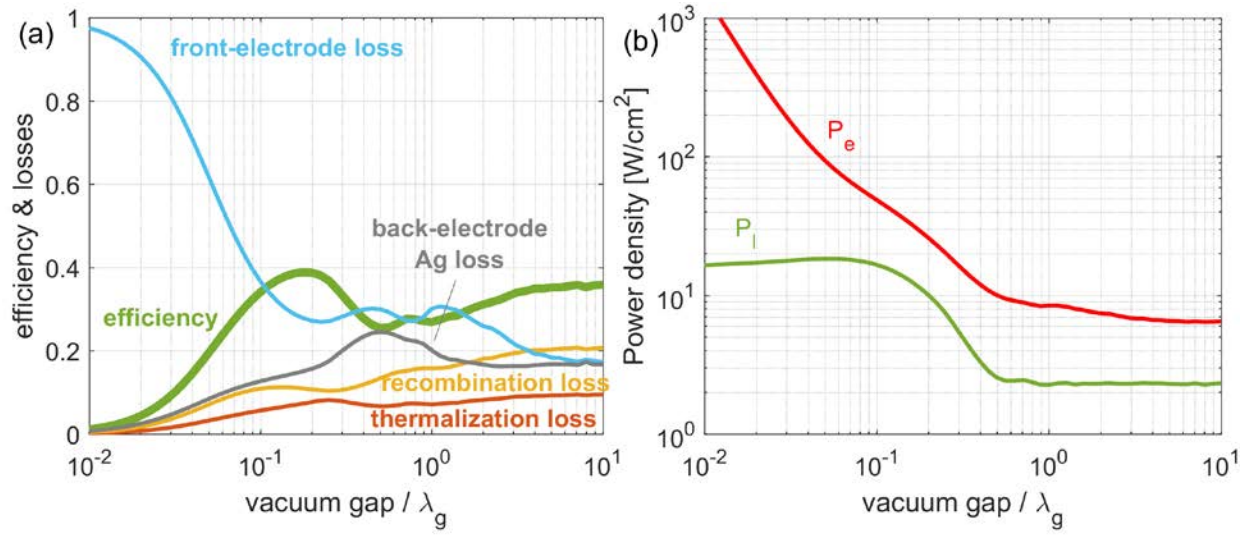

Figure 2. (a) Efficiency and losses versus vacuum gap width for TPV cell of Fig. 1(b) at doping level ω_{p1}. Efficiency rapidly drops as the two system units are brought closer together within 10s of nm, because the front electrode absorbs all the emitter thermal strongly-evanescent modes. (b) Emitted power (red) does increase as $\sim 1/d_v^2$, but output converted power (green) saturates to a smaller level. The TPV cell enters the far-field constant region for vacuum gaps roughly larger than the semiconductor band gap wavelength.

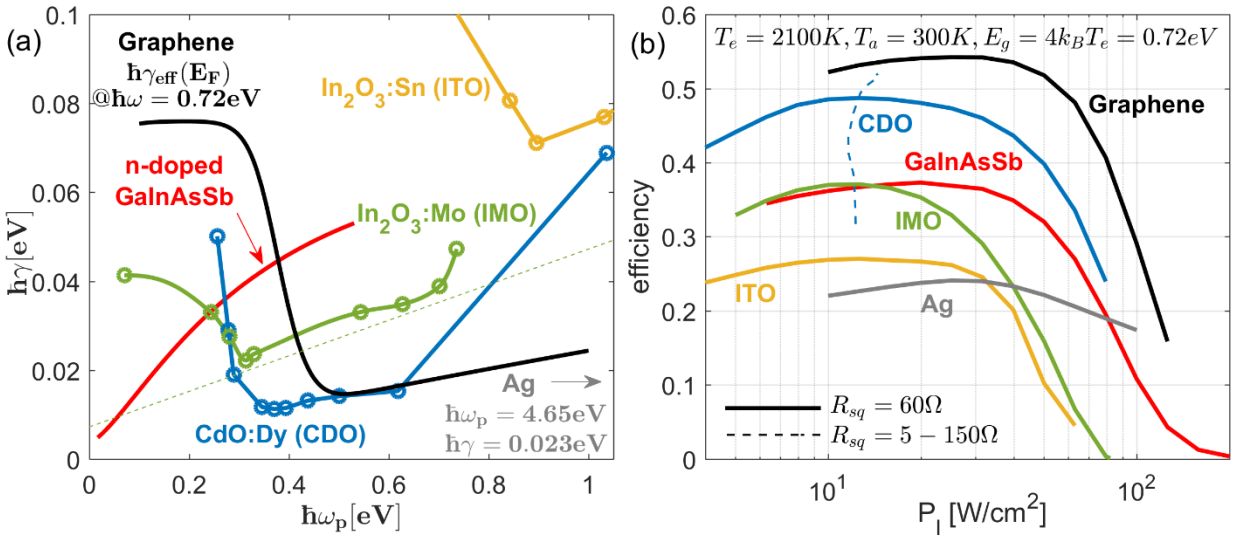

Figure 3. (a) Scattering loss rate $\gamma(\omega_p)$ (parameter quantifying losses within Drude model) as a function of plasma frequency (related to free-carrier density doping level) for a variety of material candidates for front conducting electrode. The dashed line is the heuristic loss rate used for simulations in Figs. 1 and 2. At 0.72eV, ITO and Ag are opaque to most of the incoming thermal radiation, while the other materials are transparent. (b) Efficiency comparison for materials of (a) at $T_e = 2100°K$ with $E_g = 4k_BT_e = 0.72eV$ and for $R_{sq} = 60\Omega$. The dashed blue line shows the dependence of efficiency on the necessary square resistance of a CDO electrode.

Downloaded From: https://www.spiedigitallibrary.org/conference-proceedings-of-spie on 30 Oct 2020
Terms of Use: https://www.spiedigitallibrary.org/terms-of-use

2.3 Performance comparison among several TCE materials[19]

Having understood how and why the front TCE in a TPV cell affects overall performance, it is important to evaluate the attainable TPV efficiency for different real TCE material choices. In Fig. 3(a), we show the scattering loss rate $\gamma(\omega_p)$ as a function of the plasma frequency (doping) for several material options: (1) simply doping more the cell semiconductor within a narrow top region[24], (2) indium oxide doped with either tin (ITO) or molybdenum (IMO)[25,26] and cadmium oxide doped with dysprosium (CDO)[27], (3) graphene monolayers[28,29], and (4) an ultrathin film of silver (Ag)[30].

Assuming an emitter temperature of $T_e = 2100°K$, we choose again the semiconductor band gap to be $E_g = 4k_B T_e = 0.72eV$. This means that ITO and Ag will actually be opaque to the majority of the emitted thermal field, but we saw in Fig. 1(b) that such opaque electrodes could be efficient for ultrathin cells. We compare all materials for a front-electrode square resistance of $R_{sq} = 60\Omega$, and the relative performance among materials is expected to behave similarly for other values. The results are shown in Fig. 3(b) for the efficiency as a function of desired output power (which is how all power converters should be evaluated). As one would expect, the opaque materials perform worst, although with quite decent efficiency, and the transparent materials follow the trend of their loss rates, with graphene and CDO the most efficient. The materials, whose loss rate $\gamma(\omega_p)$ has a minimum, prefer to operate at that doping level. Most importantly, the efficiency quickly drops, as the desired output power increases. The reason is that for higher power larger-wavevector modes are needed, namely, smaller vacuum gap, which leads to more losses in the TCE, as explained in Fig. 2, again counter to the general belief that in the deep near field operation both efficiency and power increase.

We also plot in Fig. 3(b) for CDO how the peak efficiency varies as a function of R_{sq} and we confirm its large influence, with peak efficiency dropping from 48% at $R_{sq} = 60\Omega$ to 32% at $R_{sq} = 5\Omega$. It is therefore very important to determine how the necessary square-resistance value depends on the metallic fingers topology.

3. METAL-GRID ELECTRODE FINGERS

3.1 Non-geometric shading losses

A grid of metallic fingers is usually printed on top of a PV cell, as shown in Fig. 4(a). The TCE conducts the photo-generated current laterally to these fingers, whose role then is to carry it along their length efficiently to the busbars. These fingers face yet another tradeoff: they would ideally be very wide, so that their resistance is very low, but no incoming radiation can penetrate through them (in other words, the fingers are shading the cell), so the wider they are the less area of the cell is used to convert radiation to electricity. In far-field (especially solar) PV cells, it is trivial to calculate these latter losses, since the calculation is purely geometric: whatever radiation hits the fingers will get reflected back and lost into infinity, so the so-called "shading" loss is the ratio of the width of a finger to the period of the fingers grid[21]. Given the fingers length, their optimal width is usually the one that balances the fingers conduction loss to the shading losses.

Let us consider now our proposed near-field TPV system with a CDO TCE, which was seen to perform well in Fig. 3(b), the width of the non-shaded part of the cell $w = 0.1mm$ and the length of the fingers $l = 0.8mm$. In Fig. 4(b), we plot the efficiency and several loss mechanisms with the ratio of widths of the fingers to the unshaded cell. The geometrically calculated shading losses $w_f/(w + w_f)$ are shown with a dashed red line, while the actual simulated ones are with solid red and are seen to be dramatically less (by a factor of 3-4). This surprising result has a very simple explanation in that, when the cell is in the close proximity of the emitter, all the thermal radiation reflected from the fingers returns to the emitter, since the view factor of the emitter to the cell is very large. Only very few grazing rays at the end of the cell will be reflected out of the emitter and lost. In different words, when the cell is within the near field of the emitter, the metal of the finger actually affects the photonic modes of the system, so that the emitter in the area across the fingers emits much less thermal power than in the area across the cell, therefore less power is eventually absorbed in the fingers and lost.

The outcome of this reduced shading loss is that, fortunately, efficiency is affected less in TPV than in regular far-field (especially) solar PV cells. Moreover, the optimal finger width, where conduction and shading losses are balanced, is much

Downloaded From: https://www.spiedigitallibrary.org/conference-proceedings-of-spie on 30 Oct 2020
Terms of Use: https://www.spiedigitallibrary.org/terms-of-use

larger than geometrical shading would indicate, as seen in Fig. 4(b), so optimal designs may typically involve larger finger-to-cell ratios.

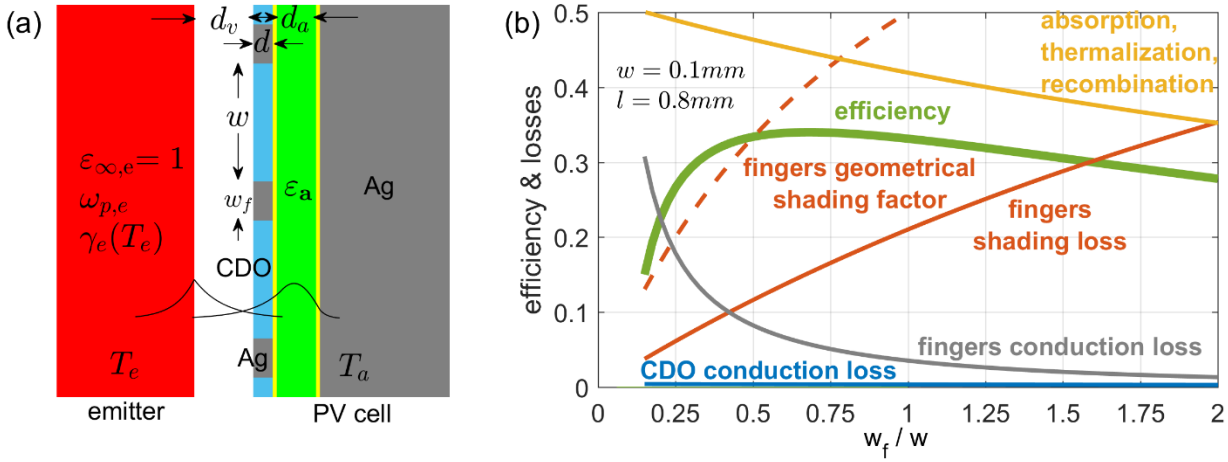

Figure 4. (a) Near-field TPV cell topology of Fig. 1(a) with metallic fingers included. Photo-generated current runs laterally through the front conducting electrode (blue) to reach the fingers (grey). (b) Efficiency and losses as a function of fingers width. Real shading losses are substantially smaller than those predicted from geometric principles, typically used for far-field PV cells. Optimal finger width, were its shading and conduction losses are balanced, is larger.

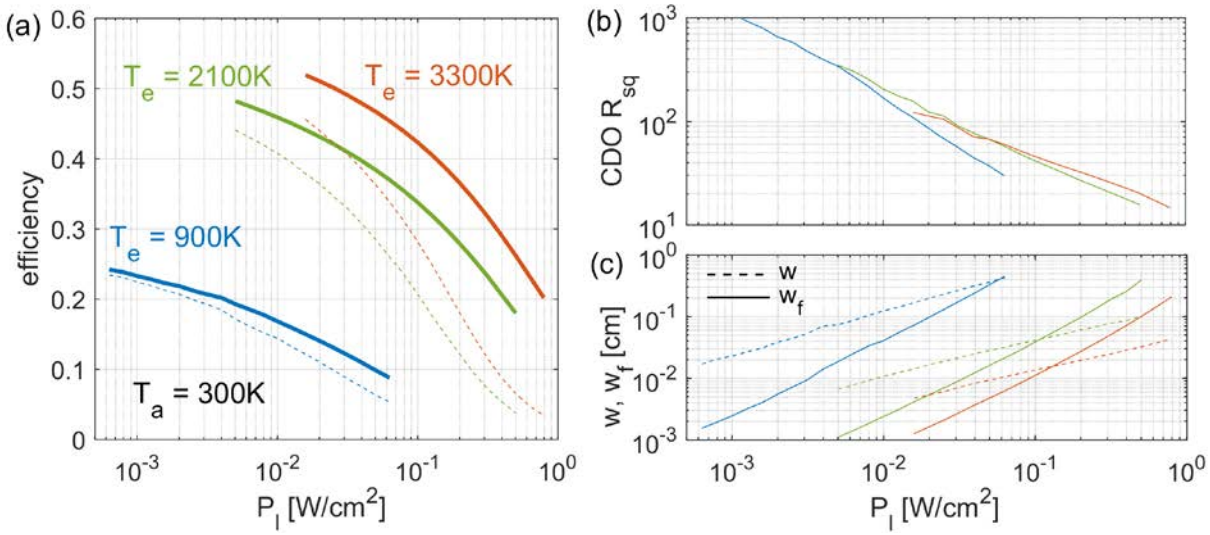

Figure 5. (a) Efficiency versus output power level for single period of TPV cell in Fig. 4(a) and for 3 different emitter temperatures. The dashed lines show the corresponding efficiencies that geometrical shading losses of the fingers would predict. (b) Corresponding optimal square resistance of the front TCE. (c) Corresponding optimal cell and finger widths. Interestingly, at very high power levels, a wider finger than the non-shaded region would be optimal.

3.2 Single finger-unit cell performance with temperature

In Fig. 3(b), it was shown that the TPV efficiency depends strongly on the TCE square resistance. Then how much square resistance is actually needed for a specific TPV cell? To answer this question, we optimize the topology of Fig. 4(a) for efficiency with respect to all system parameters. Specifically, we study how high can efficiency be, when we ask for a specific amount of output power from the part of the cell around a single metallic finger. The result is shown in Fig. 5(a) for 3 different emitter temperatures. As expected, efficiency goes down as we ask for more power and as emitter

Downloaded From: https://www.spiedigitallibrary.org/conference-proceedings-of-spie on 30 Oct 2020
Terms of Use: https://www.spiedigitallibrary.org/terms-of-use

temperature lowers. Note, however, that the gain by increasing T_e is not very large as we reach really high temperatures. If we had naively used the geometrical shading losses, the predicted efficiencies would be severely worse, especially for high temperatures. The optimal CDO square resistance is shown in Fig. 5(b) and it naturally decreases, as more power is required. Lastly, the optimal cell and finger widths are shown in Fig. 5(c); they increase in a power-law fashion with output power, but finger width increases much faster to the remarkable result that, if one were to require exceedingly large amounts of power from a singer finger unit cell, it would be preferable for the finger to be wider than the cell, for the current to be carried to the load efficiently.

4. CONCLUSIONS

We have carefully analyzed the effect of the front electrode in an ultrathin near-field TPV cell. The major conclusions are that it cannot be ignored in performance estimates, as the transparent conducting electrode heavily affects efficiency via its absorption losses, while the metallic fingers have smaller shading losses than their far-field PV cell counterparts. The design analyses indicate that a good material transparent in the infrared (such as CDO or graphene) should be used as TCE and that wider than usually fingers (or narrower than usually in-between unshaded cell regions) are better. Everything taken into consideration, the estimated results are very encouraging for potentially very efficient near-field TPV cells that also have reasonable requirements in terms of fabrication.

REFERENCES

[1] A. J. Minnich, M. S. Dresselhaus, Z. F. Ren and G. Chen, "Bulk nanostructured thermoelectric materials: current research and future prospects," *Energy Environ. Sci.* **2**, 466 (2009).

[2] Wei-Chun Hsu, Jonathan K. Tong, Bolin Liao, Yi Huang, Svetlana V. Boriskina and Gang Chen, "Entropic and Near-Field Improvements of Thermoradiative Cells," *Scientific Reports* **6**, 34837 (2016).

[3] A. Datas and A. Martí, "Thermophotovoltaic energy in space applications: Review and future potential," *Solar Energy Mat. & Solar Cells* **161**, 285 (2017).

[4] Walker R. Chan et al., "Toward high-energy-density, high-efficiency, and moderate-temperature chip-scale thermophotovoltaics," *P. Nat. Acad. Sciences* **110**, 5309 (2013).

[5] D. M. Bierman, A. Lenert, W. R. Chan, B. Bhatia, I. Celanovic, M. Soljačić and E. N. Wang, "Enhanced photovoltaic energy conversion using thermally based spectral shaping," *Nat. Energy* **1**, 1 (2016).

[6] Lu Hu, Arvind Narayanaswamy, Xiaoyuan Chen, and Gang Chen, "Near-field thermal radiation between two closely spaced glass plates exceeding Planck's blackbody radiation law," *Appl. Phys. Letters* **92**, 133106 (2008).

[7] Raphael St-Gelais, Linxiao Zhu, Shanhui Fan and Michal Lipson, "Near-field radiative heat transfer between parallel structures in the deep subwavelength regime," *Nat. Nanotechnology* **11**, 515 (2016).

[8] R. DiMatteo et al., "Micron-gap ThermoPhotoVoltaics (MTPV)," *AIP Conf. Proc., Thermophotovoltaic Generation of Electricity*, 6th (2004).

[9] M. Laroche, R. Carminati, and J.-J. Greffet, "Near-field thermophotovoltaic energy conversion," *J.Appl.Physics* **100**, 063704 (2006).

[10] Mathieu Francoeur, Rodolphe Vaillon and M. Pinar Mengüç, "Thermal Impacts on the Performance of Nanoscale-Gap Thermophotovoltaic Power Generators," *IEEE T. Energy Conv.* **26**, 686 (2011).

[11] Ognjen Ilic, Marinko Jablan, John D. Joannopoulos, Ivan Celanovic and Marin Soljačić, "Overcoming the black body limit in plasmonic and graphene near-field thermophotovoltaic systems," *Opt.Express* **20**, A366 (2012).

[12] Riccardo Messina and Philippe Ben-Abdallah, "Graphene-based photovoltaic cells for near-field thermal energy conversion," *Sci.Reports* **3**, 1383 (2013).

[13] T. J. Bright, L. P. Wang and Z. M. Zhang, "Performance of Near-Field Thermophotovoltaic Cells Enhanced With a Backside Reflector," *J. Heat Transfer* **136**, 062701 (2014).

[14] Jonathan K. Tong, Wei-Chun Hsu, Yi Huang, Svetlana V. Boriskina and Gang Chen, "Thin-film 'Thermal Well' Emitters and Absorbers for High-Efficiency Thermophotovoltaics," *Sci.Reports* **4**, 10661 (2015).

[15] Bo Zhao, Kaifeng Chen, Siddharth Buddhiraju, Gaurang Bhatt, Michal Lipson and Shanhui Fan, "High-performance near-field thermophotovoltaics for waste heat recovery," *Nano Energy* **41**, 344 (2017).

[16] T. Inoue, K. Watanabe, T. Asano and S. Noda, "Near-field thermophotovoltaic energy conversion using an intermediate transparent substrate," *Opt.Express* **26**, A192 (2018).

Downloaded From: https://www.spiedigitallibrary.org/conference-proceedings-of-spie on 30 Oct 2020
Terms of Use: https://www.spiedigitallibrary.org/terms-of-use

[17] A. Karalis and J. D. Joannopoulos, "'Squeezing' near-field thermal emission for ultra-efficient high-power thermophotovoltaic conversion," *Scientific Reports* **6**, 28472 (2016).
[18] K. A. Arpin, M. D. Losego, and P. Braun, "Electrodeposited 3D tungsten photonic crystal with enhanced thermal stability," *Chem. Mater.* **23**, 4783 (2011).
[19] A. Karalis and J. D. Joannopoulos, "Transparent and 'opaque' conducting electrodes for ultrathin highly-efficient near-field thermophotovoltaic cells," *Scientific Reports* **7**, 14046 (2017).
[20] K. Ellmer, "Past achievements and future challenges in the development of optically transparent electrodes," *Nat. Photonics* **6**, 809 (2012).
[21] M. W. Rowell and M. D.McGehee, "Transparent electrode requirements for thin film solar cell modules, " *Energy & Environmental Science* **4**, 131-134 (2011).
[22] Owen D. Miller, Steven G. Johnson and Alejandro W. Rodriguez, "Shape-Independent Limits to Near-Field Radiative Heat Transfer," *Phys. Rev. Letters* **115**, 204302 (2015).
[23] R. Vaillon et al., "Micron-sized liquid nitrogen-cooled indium antimonide photovoltaic cell for near-field thermophotovoltaics," *Opt. Express* **27**, A11 (2019).
[24] M. W. Dashiell et al., "Quaternary InGaAsSb thermophotovoltaic diodes," *IEEE Transactions on Electron Devices* **53** (12), 2879 (2006).
[25] N. Yamada et al., "Effects of postdeposition annealing on electrical properties of Mo-Doped Indium Oxide (IMO) thin films deposited by RF magnetron cosputtering," *Jap. J. of Applied Physics* **45** (44), L1179 (2006).
[26] S. Parthiban et al., "Spray deposited molybdenum doped indium oxide thin films with high near infrared transparency and carrier mobility," *Applied Physics Letters* **94** (21), 212101 (2009).
[27] E. Sachet et al., "Dysprosium-doped cadmium oxide as a gateway material for mid-infrared plasmonics," *Nat. Materials* **14**, 414 (2015).
[28] L. A. Falkovsky, "Optical properties of graphene," *J. of Physics: Conference Series* **129**, 012004 (2008).
[29] A. Pachoud et al., "Graphene transport at high carrier densities using a polymer electrolyte gate," *Europhysics Letters* **92**, 27001 (2010).
[30] W. Chen, M. D. Thoreson, S. Ishii, A. V. Kildishev and V. M.Shalaev, "Ultra-thin ultra-smooth and low-loss silver films on a germanium wetting layer," *Opt. Express* **18**, 5124 (2010).

Downloaded From: https://www.spiedigitallibrary.org/conference-proceedings-of-spie on 30 Oct 2020
Terms of Use: https://www.spiedigitallibrary.org/terms-of-use